Measurement of the $\tau^- \to \eta\pi^-\pi^+\pi^-\nu_\tau$ branching fraction and a search for a second-class current in the $\tau^- \to \eta'(958)\pi^-\nu_\tau$ decay

B. Aubert,[1] M. Bona,[1] D. Boutigny,[1] Y. Karyotakis,[1] J. P. Lees,[1] V. Poireau,[1] X. Prudent,[1] V. Tisserand,[1] A. Zghiche,[1] J. Garra Tico,[2] E. Grauges,[2] L. Lopez,[3] A. Palano,[3] M. Pappagallo,[3] G. Eigen,[4] B. Stugu,[4] L. Sun,[4] G. S. Abrams,[5] M. Battaglia,[5] D. N. Brown,[5] J. Button-Shafer,[5] R. N. Cahn,[5] Y. Groysman,[5] R. G. Jacobsen,[5] J. A. Kadyk,[5] L. T. Kerth,[5] Yu. G. Kolomensky,[5] G. Kukartsev,[5] D. Lopes Pegna,[5] G. Lynch,[5] L. M. Mir,[5] T. J. Orimoto,[5] I. L. Osipenkov,[5] M. T. Ronan,[5,*] K. Tackmann,[5] T. Tanabe,[5] W. A. Wenzel,[5] P. del Amo Sanchez,[6] C. M. Hawkes,[6] A. T. Watson,[6] H. Koch,[7] T. Schroeder,[7] D. Walker,[8] D. J. Asgeirsson,[9] T. Cuhadar-Donszelmann,[9] B. G. Fulsom,[9] C. Hearty,[9] T. S. Mattison,[9] J. A. McKenna,[9] A. Khan,[10] M. Saleem,[10] L. Teodorescu,[10] V. E. Blinov,[11] A. D. Bukin,[11] V. P. Druzhinin,[11] V. B. Golubev,[11] A. P. Onuchin,[11] S. I. Serednyakov,[11] Yu. I. Skovpen,[11] E. P. Solodov,[11] K. Yu. Todyshev,[11] M. Bondioli,[12] S. Curry,[12] I. Eschrich,[12] D. Kirkby,[12] A. J. Lankford,[12] P. Lund,[12] M. Mandelkern,[12] E. C. Martin,[12] D. P. Stoker,[12] S. Abachi,[13] C. Buchanan,[13] J. W. Gary,[14] F. Liu,[14] O. Long,[14] B. C. Shen,[14,*] G. M. Vitug,[14] L. Zhang,[14] H. P. Paar,[15] S. Rahatlou,[15] V. Sharma,[15] J. W. Berryhill,[16] C. Campagnari,[16] A. Cunha,[16] B. Dahmes,[16] T. M. Hong,[16] D. Kovalskyi,[16] J. D. Richman,[16] T. W. Beck,[17] A. M. Eisner,[17] C. J. Flacco,[17] C. A. Heusch,[17] J. Kroseberg,[17] W. S. Lockman,[17] T. Schalk,[17] B. A. Schumm,[17] A. Seiden,[17] M. G. Wilson,[17] L. O. Winstrom,[17] E. Chen,[18] C. H. Cheng,[18] F. Fang,[18] D. G. Hitlin,[18] I. Narsky,[18] T. Piatenko,[18] F. C. Porter,[18] R. Andreassen,[19] G. Mancinelli,[19] B. T. Meadows,[19] K. Mishra,[19] M. D. Sokoloff,[19] F. Blanc,[20] P. C. Bloom,[20] S. Chen,[20] W. T. Ford,[20] J. F. Hirschauer,[20] A. Kreisel,[20] M. Nagel,[20] U. Nauenberg,[20] A. Olivas,[20] J. G. Smith,[20] K. A. Ulmer,[20] S. R. Wagner,[20] J. Zhang,[20] A. M. Gabareen,[21] A. Soffer,[21,+] W. H. Toki,[21] R. J. Wilson,[21] F. Winklmeier,[21] D. D. Altenburg,[22] E. Feltresi,[22] A. Hauke,[22] H. Jasper,[22] J. Merkel,[22] A. Petzold,[22] B. Spaan,[22] K. Wacker,[22] V. Klose,[23] M. J. Kobel,[23] H. M. Lacker,[23] W. F. Mader,[23] R. Nogowski,[23] J. Schubert,[23] K. R. Schubert,[23] R. Schwierz,[23] J. E. Sundermann,[23] A. Volk,[23] D. Bernard,[24] G. R. Bonneaud,[24] E. Latour,[24] V. Lombardo,[24] Ch. Thiebaux,[24] M. Verderi,[24] P. J. Clark,[25] W. Gradl,[25] F. Muheim,[25] S. Playfer,[25] A. I. Robertson,[25] J. E. Watson,[25] Y. Xie,[25] M. Andreotti,[26] D. Bettoni,[26] C. Bozzi,[26] R. Calabrese,[26] A. Cecchi,[26] G. Cibinetto,[26] P. Franchini,[26] E. Luppi,[26] M. Negrini,[26] A. Petrella,[26] L. Piemontese,[26] E. Prencipe,[26] V. Santoro,[26] F. Anulli,[27] R. Baldini-Ferroli,[27] A. Calcaterra,[27] R. de Sangro,[27] G. Finocchiaro,[27] S. Pacetti,[27] P. Patteri,[27] I. M. Peruzzi,[27,‡] M. Piccolo,[27] M. Rama,[27] A. Zallo,[27] A. Buzzo,[28] R. Contri,[28] M. Lo Vetere,[28] M. M. Macri,[28] M. R. Monge,[28] S. Passaggio,[28] C. Patrignani,[28] E. Robutti,[28] A. Santroni,[28] S. Tosi,[28] K. S. Chaisanguanthum,[29] M. Morii,[29] J. Wu,[29] R. S. Dubitzky,[30] J. Marks,[30] S. Schenk,[30] U. Uwer,[30] D. J. Bard,[31] P. D. Dauncey,[31] R. L. Flack,[31] J. A. Nash,[31] W. Panduro Vazquez,[31] M. Tibbetts,[31] P. K. Behera,[32] X. Chai,[32] M. J. Charles,[32] U. Mallik,[32] J. Cochran,[33] H. B. Crawley,[33] L. Dong,[33] V. Eyges,[33] W. T. Meyer,[33] S. Prell,[33] E. I. Rosenberg,[33] A. E. Rubin,[33] Y. Y. Gao,[34] A. V. Gritsan,[34] Z. J. Guo,[34] C. K. Lae,[34] A. G. Denig,[35] M. Fritsch,[35] G. Schott,[35] N. Arnaud,[36] J. Béquilleux,[36] A. D'Orazio,[36] M. Davier,[36] G. Grosdidier,[36] A. Höcker,[36] V. Lepeltier,[36] F. Le Diberder,[36] A. M. Lutz,[36] S. Pruvot,[36] S. Rodier,[36] P. Roudeau,[36] M. H. Schune,[36] J. Serrano,[36] V. Sordini,[36] A. Stocchi,[36] L. Wang,[36] W. F. Wang,[36] G. Wormser,[36] D. J. Lange,[37] D. M. Wright,[37] I. Bingham,[38] J. P. Burke,[38] C. A. Chavez,[38] J. R. Fry,[38] E. Gabathuler,[38] R. Gamet,[38] D. E. Hutchcroft,[38] D. J. Payne,[38] K. C. Schofield,[38] C. Touramanis,[38] A. J. Bevan,[39] K. A. George,[39] F. Di Lodovico,[39] R. Sacco,[39] M. Sigamani,[39] G. Cowan,[40] H. U. Flaecher,[40] D. A. Hopkins,[40] S. Paramesvaran,[40] F. Salvatore,[40] A. C. Wren,[40] D. N. Brown,[41] C. L. Davis,[41] J. Allison,[42] N. R. Barlow,[42] R. J. Barlow,[42] Y. M. Chia,[42] C. L. Edgar,[42] G. D. Lafferty,[42] T. J. West,[42] J. I. Yi,[42] J. Anderson,[43] C. Chen,[43] A. Jawahery,[43] D. A. Roberts,[43] G. Simi,[43] J. M. Tuggle,[43] C. Dallapiccola,[44] S. S. Hertzbach,[44] X. Li,[44] T. B. Moore,[44] E. Salvati,[44] S. Saremi,[44] R. Cowan,[45] D. Dujmic,[45] P. H. Fisher,[45] K. Koeneke,[45] G. Sciolla,[45] M. Spitznagel,[45] F. Taylor,[45] R. K. Yamamoto,[45] M. Zhao,[45] Y. Zheng,[45] S. E. Mclachlin,[46,*] P. M. Patel,[46] S. H. Robertson,[46] A. Lazzaro,[47] F. Palombo,[47] J. M. Bauer,[48] L. Cremaldi,[48] V. Eschenburg,[48] R. Godang,[48] R. Kroeger,[48] D. A. Sanders,[48] D. J. Summers,[48] H. W. Zhao,[48] S. Brunet,[49] D. Côté,[49] M. Simard,[49] P. Taras,[49] F. B. Viaud,[49] H. Nicholson,[50] G. De Nardo,[51] F. Fabozzi,[51,§] L. Lista,[51] D. Monorchio,[51] C. Sciacca,[51] M. A. Baak,[52] G. Raven,[52] H. L. Snoek,[52] C. P. Jessop,[53] K. J. Knoepfel,[53] J. M. LoSecco,[53] G. Benelli,[54] L. A. Corwin,[54] K. Honscheid,[54] H. Kagan,[54] R. Kass,[54] J. P. Morris,[54] A. M. Rahimi,[54] J. J. Regensburger,[54] S. J. Sekula,[54] Q. K. Wong,[54] N. L. Blount,[55] J. Brau,[55] R. Frey,[55] O. Igonkina,[55] J. A. Kolb,[55] M. Lu,[55] R. Rahmat,[55] N. B. Sinev,[55] D. Strom,[55] J. Strube,[55] E. Torrence,[55] N. Gagliardi,[56] A. Gaz,[56] M. Margoni,[56] M. Morandin,[56] A. Pompili,[56] M. Posocco,[56] M. Rotondo,[56] F. Simonetto,[56] R. Stroili,[56] C. Voci,[56] E. Ben-Haim,[57] H. Briand,[57] G. Calderini,[57] J. Chauveau,[57] P. David,[57] L. Del Buono,[57] Ch. de la Vaissière,[57] O. Hamon,[57] Ph. Leruste,[57] J. Malclès,[57] J. Ocariz,[57] A. Perez,[57] J. Prendki,[57] L. Gladney,[58] M. Biasini,[59] R. Covarelli,[59] E. Manoni,[59] C. Angelini,[60] G. Batignani,[60]

S. Bettarini,[60] M. Carpinelli,[60,‖] R. Cenci,[60] A. Cervelli,[60] F. Forti,[60] M. A. Giorgi,[60] A. Lusiani,[60] G. Marchiori,[60] M. A. Mazur,[60] M. Morganti,[60] N. Neri,[60] E. Paoloni,[60] G. Rizzo,[60] J. J. Walsh,[60] J. Biesiada,[61] P. Elmer,[61] Y. P. Lau,[61] C. Lu,[61] J. Olsen,[61] A. J. S. Smith,[61] A. V. Telnov,[61] E. Baracchini,[62] F. Bellini,[62] G. Cavoto,[62] D. del Re,[62] E. Di Marco,[62] R. Faccini,[62] F. Ferrarotto,[62] F. Ferroni,[62] M. Gaspero,[62] P. D. Jackson,[62] M. A. Mazzoni,[62] S. Morganti,[62] G. Piredda,[62] F. Polci,[62] F. Renga,[62] C. Voena,[62] M. Ebert,[63] T. Hartmann,[63] H. Schröder,[63] R. Waldi,[63] T. Adye,[64] G. Castelli,[64] B. Franek,[64] E. O. Olaiya,[64] W. Roethel,[64] F. F. Wilson,[64] S. Emery,[65] M. Escalier,[65] A. Gaidot,[65] S. F. Ganzhur,[65] G. Hamel de Monchenault,[65] W. Kozanecki,[65] G. Vasseur,[65] Ch. Yèche,[65] M. Zito,[65] X. R. Chen,[66] H. Liu,[66] W. Park,[66] M. V. Purohit,[66] R. M. White,[66] J. R. Wilson,[66] M. T. Allen,[67] D. Aston,[67] R. Bartoldus,[67] P. Bechtle,[67] R. Claus,[67] J. P. Coleman,[67] M. R. Convery,[67] J. C. Dingfelder,[67] J. Dorfan,[67] G. P. Dubois-Felsmann,[67] W. Dunwoodie,[67] R. C. Field,[67] T. Glanzman,[67] S. J. Gowdy,[67] M. T. Graham,[67] P. Grenier,[67] C. Hast,[67] W. R. Innes,[67] J. Kaminski,[67] M. H. Kelsey,[67] H. Kim,[67] P. Kim,[67] M. L. Kocian,[67] D. W. G. S. Leith,[67] S. Li,[67] S. Luitz,[67] V. Luth,[67] H. L. Lynch,[67] D. B. MacFarlane,[67] H. Marsiske,[67] R. Messner,[67] D. R. Muller,[67] S. Nelson,[67] C. P. O'Grady,[67] I. Ofte,[67] A. Perazzo,[67] M. Perl,[67] T. Pulliam,[67] B. N. Ratcliff,[67] A. Roodman,[67] A. A. Salnikov,[67] R. H. Schindler,[67] J. Schwiening,[67] A. Snyder,[67] D. Su,[67] M. K. Sullivan,[67] S. Sun,[67] K. Suzuki,[67] S. K. Swain,[67] J. M. Thompson,[67] J. Va'vra,[67] A. P. Wagner,[67] M. Weaver,[67] W. J. Wisniewski,[67] M. Wittgen,[67] D. H. Wright,[67] A. K. Yarritu,[67] K. Yi,[67] C. C. Young,[67] V. Ziegler,[67] P. R. Burchat,[68] A. J. Edwards,[68] S. A. Majewski,[68] T. S. Miyashita,[68] B. A. Petersen,[68] L. Wilden,[68] S. Ahmed,[69] M. S. Alam,[69] R. Bula,[69] J. A. Ernst,[69] B. Pan,[69] M. A. Saeed,[69] F. R. Wappler,[69] S. B. Zain,[69] S. M. Spanier,[70] B. J. Wogsland,[70] R. Eckmann,[71] J. L. Ritchie,[71] A. M. Ruland,[71] C. J. Schilling,[71] R. F. Schwitters,[71] J. M. Izen,[72] X. C. Lou,[72] S. Ye,[72] F. Bianchi,[73] F. Gallo,[73] D. Gamba,[73] M. Pelliccioni,[73] M. Bomben,[74] L. Bosisio,[74] C. Cartaro,[74] F. Cossutti,[74] G. Della Ricca,[74] L. Lanceri,[74] L. Vitale,[74] V. Azzolini,[75] N. Lopez-March,[75] F. Martinez-Vidal,[75,¶] D. A. Milanes,[75] A. Oyanguren,[75] J. Albert,[76] Sw. Banerjee,[76] B. Bhuyan,[76] K. Hamano,[76] R. Kowalewski,[76] M. Lewczuk,[76] I. M. Nugent,[76] J. M. Roney,[76] R. J. Sobie,[76] P. F. Harrison,[77] J. Ilic,[77] T. E. Latham,[77] G. B. Mohanty,[77] H. R. Band,[78] X. Chen,[78] S. Dasu,[78] K. T. Flood,[78] J. J. Hollar,[78] P. E. Kutter,[78] Y. Pan,[78] M. Pierini,[78] R. Prepost,[78] S. L. Wu,[78] and H. Neal[79]

(*BABAR* Collaboration)

[1]*Laboratoire de Physique des Particules, IN2P3/CNRS et Université de Savoie, F-74941 Annecy-Le-Vieux, France*
[2]*Universitat de Barcelona, Facultat de Fisica, Departament ECM, E-08028 Barcelona, Spain*
[3]*Università di Bari, Dipartimento di Fisica and INFN, I-70126 Bari, Italy*
[4]*University of Bergen, Institute of Physics, N-5007 Bergen, Norway*
[5]*Lawrence Berkeley National Laboratory and University of California, Berkeley, California 94720, USA*
[6]*University of Birmingham, Birmingham B15 2TT, United Kingdom*
[7]*Ruhr Universität Bochum, Institut für Experimentalphysik 1, D-44780 Bochum, Germany*
[8]*University of Bristol, Bristol BS8 1TL, United Kingdom*
[9]*University of British Columbia, Vancouver, British Columbia, Canada V6T 1Z1*
[10]*Brunel University, Uxbridge, Middlesex UB8 3PH, United Kingdom*
[11]*Budker Institute of Nuclear Physics, Novosibirsk 630090, Russia*
[12]*University of California at Irvine, Irvine, California 92697, USA*
[13]*University of California at Los Angeles, Los Angeles, California 90024, USA*
[14]*University of California at Riverside, Riverside, California 92521, USA*
[15]*University of California at San Diego, La Jolla, California 92093, USA*
[16]*University of California at Santa Barbara, Santa Barbara, California 93106, USA*
[17]*University of California at Santa Cruz, Institute for Particle Physics, Santa Cruz, California 95064, USA*
[18]*California Institute of Technology, Pasadena, California 91125, USA*
[19]*University of Cincinnati, Cincinnati, Ohio 45221, USA*
[20]*University of Colorado, Boulder, Colorado 80309, USA*
[21]*Colorado State University, Fort Collins, Colorado 80523, USA*
[22]*Universität Dortmund, Institut für Physik, D-44221 Dortmund, Germany*
[23]*Technische Universität Dresden, Institut für Kern-und Teilchenphysik, D-01062 Dresden, Germany*
[24]*Laboratoire Leprince-Ringuet, CNRS/IN2P3, Ecole Polytechnique, F-91128 Palaiseau, France*
[25]*University of Edinburgh, Edinburgh EH9 3JZ, United Kingdom*
[26]*Università di Ferrara, Dipartimento di Fisica and INFN, I-44100 Ferrara, Italy*
[27]*Laboratori Nazionali di Frascati dell'INFN, I-00044 Frascati, Italy*
[28]*Università di Genova, Dipartimento di Fisica and INFN, I-16146 Genova, Italy*
[29]*Harvard University, Cambridge, Massachusetts 02138, USA*
[30]*Universität Heidelberg, Physikalisches Institut, Philosophenweg 12, D-69120 Heidelberg, Germany*

[31]Imperial College London, London SW7 2AZ, United Kingdom
[32]University of Iowa, Iowa City, Iowa 52242, USA
[33]Iowa State University, Ames, Iowa 50011-3160, USA
[34]Johns Hopkins University, Baltimore, Maryland 21218, USA
[35]Universität Karlsruhe, Institut für Experimentelle Kernphysik, D-76021 Karlsruhe, Germany
[36]Laboratoire de l'Accélérateur Linéaire, IN2P3/CNRS et Université Paris-Sud 11, Centre Scientifique d'Orsay, B. P. 34, F-91898 ORSAY Cedex, France
[37]Lawrence Livermore National Laboratory, Livermore, California 94550, USA
[38]University of Liverpool, Liverpool L69 7ZE, United Kingdom
[39]Queen Mary, University of London, E1 4NS, United Kingdom
[40]University of London, Royal Holloway and Bedford New College, Egham, Surrey TW20 0EX, United Kingdom
[41]University of Louisville, Louisville, Kentucky 40292, USA
[42]University of Manchester, Manchester M13 9PL, United Kingdom
[43]University of Maryland, College Park, Maryland 20742, USA
[44]University of Massachusetts, Amherst, Massachusetts 01003, USA
[45]Massachusetts Institute of Technology, Laboratory for Nuclear Science, Cambridge, Massachusetts 02139, USA
[46]McGill University, Montréal, Québec, Canada H3A 2T8
[47]Università di Milano, Dipartimento di Fisica and INFN, I-20133 Milano, Italy
[48]University of Mississippi, University, Mississippi 38677, USA
[49]Université de Montréal, Physique des Particules, Montréal, Québec, Canada H3C 3J7
[50]Mount Holyoke College, South Hadley, Massachusetts 01075, USA
[51]Università di Napoli Federico II, Dipartimento di Scienze Fisiche and INFN, I-80126, Napoli, Italy
[52]National Institute for Nuclear Physics and High Energy Physics (NIKHEF), NL-1009 DB Amsterdam, The Netherlands
[53]University of Notre Dame, Notre Dame, Indiana 46556, USA
[54]Ohio State University, Columbus, Ohio 43210, USA
[55]University of Oregon, Eugene, Oregon 97403, USA
[56]Università di Padova, Dipartimento di Fisica and INFN, I-35131 Padova, Italy
[57]Laboratoire de Physique Nucléaire et de Hautes Energies, IN2P3/CNRS, Université Pierre et Marie Curie-Paris 6, Université Denis Diderot-Paris 7, F-75252 Paris, France
[58]University of Pennsylvania, Philadelphia, Pennsylvania 19104, USA
[59]Università di Perugia, Dipartimento di Fisica and INFN, I-06100 Perugia, Italy
[60]Università di Pisa, Dipartimento di Fisica, Scuola Normale Superiore and INFN, I-56127 Pisa, Italy
[61]Princeton University, Princeton, New Jersey 08544, USA
[62]Università di Roma La Sapienza, Dipartimento di Fisica and INFN, I-00185 Roma, Italy
[63]Universität Rostock, D-18051 Rostock, Germany
[64]Rutherford Appleton Laboratory, Chilton, Didcot, Oxon, OX11 0QX, United Kingdom
[65]DSM/Dapnia, CEA/Saclay, F-91191 Gif-sur-Yvette, France
[66]University of South Carolina, Columbia, South Carolina 29208, USA
[67]Stanford Linear Accelerator Center, Stanford, California 94309, USA
[68]Stanford University, Stanford, California 94305-4060, USA
[69]State University of New York, Albany, New York 12222, USA
[70]University of Tennessee, Knoxville, Tennessee 37996, USA
[71]University of Texas at Austin, Austin, Texas 78712, USA
[72]University of Texas at Dallas, Richardson, Texas 75083, USA
[73]Università di Torino, Dipartimento di Fisica Sperimentale and INFN, I-10125 Torino, Italy
[74]Università di Trieste, Dipartimento di Fisica and INFN, I-34127 Trieste, Italy
[75]IFIC, Universitat de Valencia-CSIC, E-46071 Valencia, Spain
[76]University of Victoria, Victoria, British Columbia, Canada V8W 3P6
[77]Department of Physics, University of Warwick, Coventry CV4 7AL, United Kingdom
[78]University of Wisconsin, Madison, Wisconsin 53706, USA
[79]Yale University, New Haven, Connecticut 06511, USA
(Received 14 March 2008; published 10 June 2008)

[*]Deceased
[+]Now at Tel Aviv University, Tel Aviv 69978, Israel
[‡]Also with Università di Perugia, Dipartimento di Fisica, Perugia, Italy
[§]Also with Università della Basilicata, Potenza, Italy
[‖]Also with Università di Sassari, Sassari, Italy
[¶]Also with Universitat de Barcelona, Facultat de Fisica, Departament ECM, E-08028 Barcelona, Spain

The $\tau^- \to \eta\pi^-\pi^+\pi^-\nu_\tau$ decay with the $\eta \to \gamma\gamma$ mode is studied using 384 fb^{-1} of data collected by the *BABAR* detector. The branching fraction is measured to be $(1.60 \pm 0.05 \pm 0.11) \times 10^{-4}$. It is found that $\tau^- \to f_1(1285)\pi^-\nu_\tau \to \eta\pi^-\pi^+\pi^-\nu_\tau$ is the dominant decay mode with a branching fraction of $(1.11 \pm 0.06 \pm 0.05) \times 10^{-4}$. The first error on the branching fractions is statistical and the second systematic. Note that no particle identification algorithm is applied to the charged tracks to distinguish pions from kaons. In addition, a 90% confidence level upper limit on the branching fraction of the $\tau^- \to \eta'(958)\pi^-\nu_\tau$ decay is measured to be 7.2×10^{-6}. This last decay proceeds through a second-class current and is expected to be forbidden in the limit of isospin symmetry.

DOI: 10.1103/PhysRevD.77.112002 PACS numbers: 13.35.Dx, 14.60.Fg

I. INTRODUCTION

The high-statistics sample of τ-pair events collected by the *BABAR* experiment allows detailed studies of τ-lepton decays with small branching fractions. Many of these decays are poorly understood and more precise measurements of the branching fractions as well as studies of the decay mechanisms are required. This work examines the $\tau^- \to \eta\pi^-\pi^+\pi^-\nu_\tau$ decay [1] where $\eta \to \gamma\gamma$. We show that this mode is dominated by $\tau^- \to f_1(1285)\pi^-\nu_\tau$. This decay mode has been previously studied by the CLEO Collaboration [2]. A measurement of the $\tau^- \to f_1(1285)\pi^-\nu_\tau$ decay was also made by the *BABAR* Collaboration, using the $f_1(1285) \to 2\pi^+2\pi^-$ decay mode [3].

This work also presents a search for the $\tau^- \to \eta'(958)\pi^-\nu_\tau$ decay where $\eta'(958) \to \eta\pi^-\pi^+$. Since this τ decay proceeds via a second-class current, it is expected to be forbidden in the case of isospin symmetry. A 90% confidence level upper limit has been previously set by the CLEO Collaboration at 7.4×10^{-5} [2].

This analysis is based on data recorded by the *BABAR* detector at the PEP-II asymmetric-energy e^+e^- storage rings operated at the Stanford Linear Accelerator Center. The data sample corresponds to an integrated luminosity of 384 fb^{-1} recorded at center-of-mass energies of 10.58 GeV and 10.54 GeV between 1999 and 2006. With a cross section for $e^+e^- \to \tau^+\tau^-$ production of (0.919 ± 0.003) nb [4], this data sample contains approximately 7.06×10^8 τ decays.

The *BABAR* detector is described in detail in Ref. [5]. Charged particle momenta are measured with a five-layer double-sided silicon vertex tracker and a 40-layer drift chamber inside a 1.5-T superconducting solenoidal magnet. A detector of internally reflected Cherenkov light (DIRC) provides π/K separation. A calorimeter consisting of CsI (Tl) crystals is used to measure the energy of electromagnetic showers, and an instrumented magnetic flux return (IFR) is used to identify muons.

Monte Carlo simulation is used to evaluate the background contamination and selection efficiencies. The τ-pair production is simulated with the KK2F Monte Carlo event generator [6]. The τ decays, continuum $q\bar{q}$ events, and final-state radiative effects are modeled with TAUOLA [7], JETSET [8], and PHOTOS [9], respectively. The generic τ Monte Carlo sample contains one decay mode with an η meson in the final state, $\tau^- \to \eta\pi^-\pi^0\nu_\tau$. In addition, a dedicated Monte Carlo sample is generated using KK2F and TAUOLA for the $\tau^- \to \eta K_s^0\pi^-\nu_\tau$ decay.

Dedicated samples of $\tau^+\tau^-$ events are created using EVTGEN [10] where one of the τ leptons can decay to any mode included in TAUOLA [7] and the other τ decays to an $\eta\pi^-\pi^+\pi^-\nu_\tau$ final state. One of the samples is generated using the $\tau^- \to f_1(1285)\pi^-\nu_\tau$ decay and the other is generated using $\tau^- \to \eta\pi^-\pi^+\pi^-\nu_\tau$ phase space. The $f_1(1285)$ meson decays relevant to this analysis are the $f_1(1285) \to \eta\pi^-\pi^+$ and the $f_1(1285) \to a_0(980)\pi$ decay modes. The Monte Carlo distributions identified as signal in the figures use a combination of $\tau^- \to \eta\pi^-\pi^+\pi^-\nu_\tau$ phase space and the resonant $\tau^- \to f_1(1285)\pi^-\nu_\tau$ decay samples where the relative fraction is based on the branching fractions measured in this work.

The detector response is simulated with GEANT4 [11]. All Monte Carlo simulation events are passed through a full simulation of the *BABAR* detector and are reconstructed in the same way as the data [5].

II. SELECTION

Events of interest are isolated with a loose preselection. Since τ pairs are produced back-to-back in the e^+e^- center-of-mass frame, the event is divided into hemispheres according to the thrust axis [12], calculated using all reconstructed charged and neutral particles. The analysis procedure selects events with one track in one hemisphere (tag hemisphere) and three tracks in the other hemisphere (signal hemisphere). The total event charge is required to be zero.

Charged particles are required to have transverse momenta greater than 0.1 GeV/c in the laboratory frame. The distance of the point of closest approach of the track to the beam axis must be less than 1.5 cm. In addition, the z coordinate (along the beam axis) of the point of closest approach of the track must be within 10 cm of the z coordinate of the production point. Neutral clusters are required to have an energy of at least 30 MeV and must not be associated with a charged track.

After preselection a more discriminating analysis selection is applied. This selection strategy has three components. The first selection criterion is based on the

event-shape properties. The magnitude of the thrust is required to be between 0.92 and 0.99, in order to reduce the non-τ backgrounds. The background from non-τ sources can arise from Bhabha, di-muon, two-photon, and $q\bar{q}$ events.

The second set of selection criteria requires the particles in the tag hemisphere to originate from a leptonic τ decay ($\tau^- \to e^- \nu\bar{\nu}$ or $\tau^- \to \mu^- \nu\bar{\nu}$). The track in the tag hemisphere must be identified as an electron or muon and must have a momentum in the center-of-mass frame below 4 GeV/c. The first criterion removes $q\bar{q}$ events while the second removes lepton-pair events. Electrons are identified with the use of the ratio of energy measured by the calorimeter to track momentum (E/p), the ionization loss in the tracking system (dE/dx), and the shape of the shower in the calorimeter. Muons are identified by hits in the IFR and energy deposits in the calorimeter expected for a minimum-ionizing particle. Residual background from $q\bar{q}$ events is reduced by requiring that there be at most one electromagnetic calorimeter cluster in the tag hemisphere with energy above 50 MeV and that the total neutral energy in the tag hemisphere be less than 1 GeV.

The final set of selection criteria is applied to the signal hemisphere. The aim is to reduce the residual backgrounds from τ decays while maintaining high selection efficiency for $\tau^- \to \eta\pi^-\pi^+\pi^-\nu_\tau$ decays. An event is rejected if any of the tracks in the signal hemisphere is identified as an electron or if any pair of oppositely charged tracks is consistent with originating from a photon conversion.

The event selection requires that there be one unique $\eta \to \gamma\gamma$ candidate in the signal hemisphere. The $\eta \to \gamma\gamma$ candidates consist of two neutral clusters in the electromagnetic calorimeter with an invariant mass ($M_{\gamma\gamma}$) between 0.47 and 0.62 GeV/c^2. To reduce combinatoric background from other τ decays with π^0 mesons, the higher- and lower-energy clusters must have $E > 0.7$ GeV and $E > 0.3$ GeV, respectively.

Residual background from other τ decays and $q\bar{q}$ events is reduced by requiring that there be no π^0 mesons in the signal hemisphere, where a π^0 candidate consists of two neutral clusters in the electromagnetic calorimeter with an invariant $\gamma\gamma$ mass between 115 and 150 MeV/c^2. In addition the invariant mass of the $\eta\pi^-\pi^+\pi^-$ system is required to be less than 1.8 GeV/c^2. No particle identification algorithm is applied to the charged tracks to distinguish pions from kaons, and all invariant masses are calculated assuming that the charged particles are pions. Note that the $\tau^- \to f_1(1285)K^-\nu_\tau$ decay is kinematically disfavored. Monte Carlo studies indicate that the background from τ decays is dominated by $\gamma\gamma$ combinatorics in the $\pi^-\pi^+\pi^-(\geq 1\pi^0)$ mode. The absolute amount of τ background is determined in the fits. The backgrounds from $\tau^- \to \eta K^0_S \pi^- \nu_\tau$ and $q\bar{q}$ are evaluated separately and discussed in Sec. III.

III. RESULTS

The invariant mass of the η candidates is shown in Fig. 1 (a) after all selection criteria are applied. The plot shows a difference in the reconstructed mass and width of the η meson between the data and Monte Carlo simulation. The width of the η peak obtained in a fit using only the signal Monte Carlo sample was slightly narrower but consistent with the width from the data. The variations in the fit results between data and signal Monte Carlo are accounted for with a systematic error discussed in the following section.

Figure 1(b) shows the invariant mass of the $\eta\pi^-\pi^+\pi^-$ system after all selection criteria (except on this variable) have been applied. The disagreement between the data and Monte Carlo simulation in Fig. 1(b) shows that the underlying physics is more complex than the model used to simulate the decay and may involve additional reso-

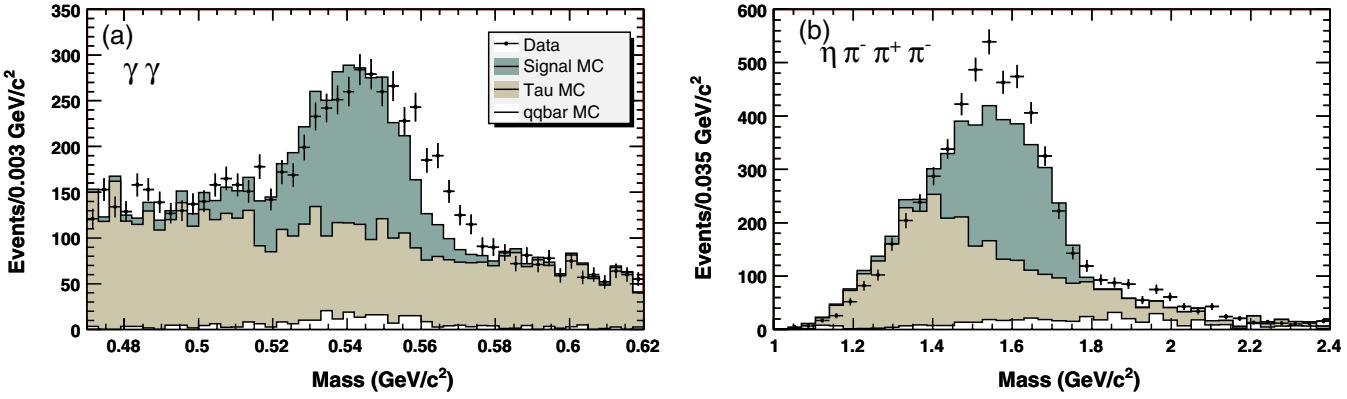

FIG. 1 (color online). The invariant masses of the (a) $\gamma\gamma$, and (b) $\eta\pi^-\pi^+\pi^-$ final states are shown. The dark shaded histograms show the simulated signal events, the lightly shaded histograms show the simulated τ background, and the unshaded histograms show the simulated $q\bar{q}$ background. All selection criteria are applied. In (b) the cut requirement on the invariant mass of the $\eta\pi^-\pi^+\pi^-$ system is not imposed and the invariant mass of the $\gamma\gamma$ system is between 0.50 and 0.58 GeV/c^2.

nances. For example the model used in TAUOLA for the $\tau \to 3\pi 2\pi^0 \nu_\tau$ mode, does not give an accurate representation of the experimental data [13]. However, the $\eta\pi^-\pi^+\pi^-$ invariant mass distribution is not used in the determination of the branching fractions presented in this paper and the modeling uncertainties are small and included in the systematic errors.

Figure 2(a) shows the invariant mass of the $\eta\pi^-\pi^+$ system. Figure 2(b) shows the invariant mass of the $\eta\pi^-$ and $\eta\pi^+$ systems with the requirement that the invariant mass of the $\eta\pi^-\pi^+$ system is between 1.23 and 1.32 GeV/c^2 [consistent with being an $f_1(1285)$ meson]. Only the π mesons forming the $f_1(1285)$ candidates are shown in this plot. The peak at 980 MeV/c^2 is due to the $a_0(980)$ in the $f_1(1285) \to a_0(980)\pi$ decay.

A. Inclusive $\tau^- \to \eta\pi^-\pi^+\pi^-\nu_\tau$ branching fraction

The invariant mass distribution of the $\gamma\gamma$ system is fitted with a Novosibirsk function [14] (Gaussian distribution with a tail parameter) for the η meson plus a polynomial function for the background. The fit range is 0.47 to 0.62 GeV/c^2 and the fit is a binned χ^2 fit. The observed width of the η is dominated by the experimental resolution (14 MeV/c^2). The resolution and the tail parameters in the fit to the data are fixed to the values obtained from a fit to the signal Monte Carlo simulation (see the following paragraphs for a discussion of the systematic error associated with this constraint). The peak position and normalization parameters of the Novosibirsk function are allowed to vary in the fit to minimize the dependence of the result on the difference in the η mass observed between the data and Monte Carlo simulation.

A total of 2174 ± 73 events is obtained from the fit shown in Fig. 3(a). The χ^2 per number of degrees of freedom for the fit is 51/46.

The $\tau^- \to \eta\pi^-\pi^+\pi^-\nu_\tau$ branching fraction is measured with

$$B_{\tau^- \to \eta\pi^-\pi^+\pi^-\nu_\tau} = \frac{N_{\rm obs} - N_{\rm bkgd}}{2N_{\tau^+\tau^-}} \frac{1}{\epsilon} \frac{1}{B(\eta \to \gamma\gamma)}, \quad (1)$$

where $N_{\rm obs}$ is the number of events obtained from the fit, $N_{\rm bkgd}$ is the number of background events with an η meson (371 ± 83), $N_{\tau^+\tau^-}$ is the number of τ leptons in the sample calculated from the luminosity and $e^+e^- \to \tau^+\tau^-$ cross section, ϵ is the efficiency for selecting the signal events ($4.18 \pm 0.06\%$), and $B(\eta \to \gamma\gamma)$ is 0.3943 ± 0.0026 [15]. The $\tau^- \to \eta\pi^-\pi^+\pi^-\nu_\tau$ branching fraction is measured to be $(1.60 \pm 0.05 \pm 0.11) \times 10^{-4}$ where the first error is statistical and the second is systematic.

The systematic errors are dominated by the uncertainty in the results of the fit to the η meson (5.0%), which is partly due to the difference in the $\gamma\gamma$ mass resolutions in the data and Monte Carlo. The sensitivity of the results to the fit to the η peak is investigated by unconstraining the width and tail parameters in the fit to the data. Also, polynomials of different orders are tested as background functions. The 5.0% uncertainty associated with the fit is also due partly to the variation of the branching fraction observed for different background functions. The remaining systematic errors include terms for the uncertainties of the η background levels (3.8%), η selection efficiency (3.0%), track reconstruction (2.4%), lepton identification (1.6%), selection efficiency statistical error (1.4%), luminosity (1.0%), and the $\eta \to \gamma\gamma$ branching fraction (0.7%).

The background events ($N_{\rm bkgd}$) include a contribution from $q\bar{q}$ events which is estimated from $q\bar{q}$ Monte Carlo samples. The uncertainty in the number of background events extracted from the $q\bar{q}$ background is evaluated by comparing data and Monte Carlo simulation distributions in regions where there is an enhanced amount of $q\bar{q}$ events (events with an $\eta\pi^-\pi^+\pi^-$ invariant mass that is larger

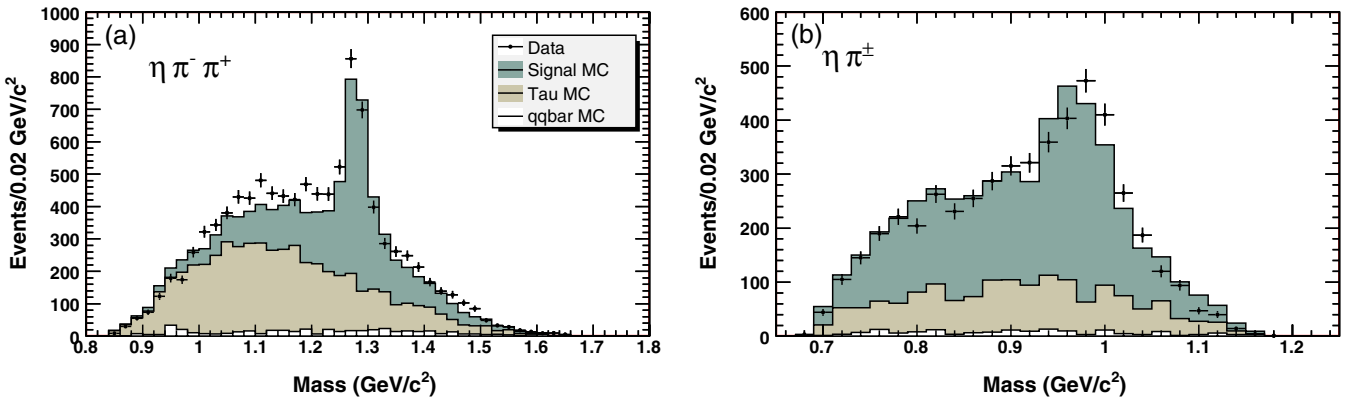

FIG. 2 (color online). The invariant masses of the (a) $\eta\pi^-\pi^+$ and (b) $\eta\pi^\pm$ final states are shown. The dark shaded histograms show the simulated signal events, the lightly shaded histograms show the simulated τ background, and the unshaded histograms show the simulated $q\bar{q}$ background. Note that (a) and (b) have two entries per event. All selection criteria are applied. In (b), it is required that the invariant mass of the associated $\eta\pi^-\pi^+$ system is between 1.23 and 1.32 GeV/c^2.

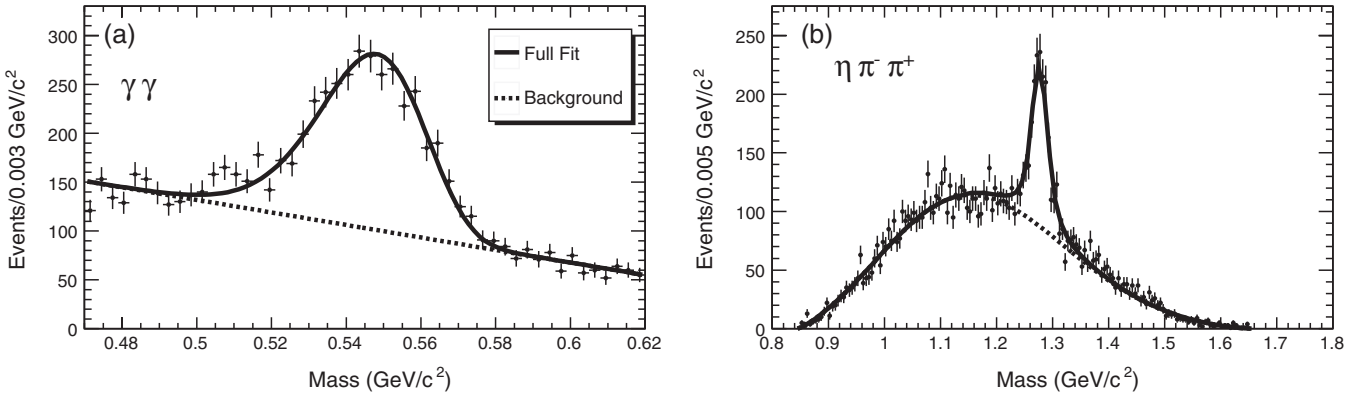

FIG. 3. Plot (a) shows the invariant mass of the $\gamma\gamma$ system. Plot (b) shows the invariant mass of the data $\eta\pi^-\pi^+$ system. The points represent the data, the solid line is the fit function, and the dashed line shows the background.

than the τ mass). The $q\bar{q}$ Monte Carlo predicts 125 candidates with an η meson with an uncertainty of 18 events.

The background also gets a contribution from $\tau^- \to \eta K_S^0 \pi^- \nu_\tau$ events. The number of K_S^0 candidates is determined by counting the number of events that pass the full selection from the dedicated $\tau^- \to \eta K_S^0 \pi^- \nu_\tau$ Monte Carlo. The Monte Carlo predicts 246 K_S^0 background events. The uncertainty on the number of selected background events is dominated by the uncertainty of the $\tau^- \to \eta K_S^0 \pi^- \nu_\tau$ branching fraction $B_{\tau^- \to \eta K_S^0 \pi^- \nu_\tau} = (1.10 \pm 0.35 \pm 0.11) \times 10^{-4}$ [16]. The total background is estimated to be $N_{\rm bkgd} = 371 \pm 83$ where the uncertainties from the $q\bar{q}$ and K_S^0 backgrounds are added in quadrature and included as a systematic error.

The stability of the branching fraction measurements was tested by varying the selection criteria (within a range of values determined by the level of agreement between data and Monte Carlo), which did not change the results significantly. Furthermore, the results of the fit to the η meson mass peak are found to be stable to variations in the bin width or mass range used in the fit. Branching fractions measured on the electron and muon samples separately are found to be consistent.

B. Branching fractions for $\tau^- \to f_1(1285)\pi^-\nu_\tau \to \eta\pi^-\pi^+\pi^-\nu_\tau$ and $\tau^- \to f_1(1285)\pi^-\nu_\tau$

The $f_1(1285)\pi$ candidates are selected with the criteria specified in the previous section with the requirement that the η candidates have $0.50 < M_{\gamma\gamma} < 0.58$ GeV/c^2. The invariant mass of the $\eta\pi^-\pi^+$ system is fitted with a Breit-Wigner function convoluted with a Gaussian distribution and the background is modeled with a Novosibirsk function summed with a polynomial [see Fig. 3(b)]. The χ^2 per number of degrees of freedom is 180/152 for the $\eta\pi^-\pi^+$ fit. A P-wave Breit-Wigner function [17] is used to fit the data while the fit to the simulated distribution uses a simple Breit-Wigner function as implemented in the generator. In both cases the Breit-Wigner function is modulated by phase space. The normalization and mean of the Breit-Wigner function are allowed to vary and the width is fixed to the world average. The resolution parameter of the Gaussian function is fixed to 7 MeV/c^2, which is the mass resolution of the $\eta\pi^-\pi^+$ system obtained from simulation.

The background function is determined by fitting the $\eta\pi^-\pi^+$ invariant mass distribution obtained from a sample of simulated $\tau^- \to \eta\pi^-\pi^+\pi^-\nu_\tau$ events where the decay does not proceed through an $f_1(1285)$ meson.

There is no evidence for the production of $f_1(1285)$ mesons in the data from background sources. This is determined by relaxing selection criteria to increase the background from multihadron events.

The $\tau^- \to f_1(1285)\pi^-\nu_\tau \to \eta\pi^-\pi^+\pi^-\nu_\tau$ branching fraction is determined with

$$B_{\tau^- \to \eta\pi^-\pi^+\pi^-\nu_\tau(\text{via } f_1)} = \frac{N_{\rm obs}}{2N_{\tau^+\tau^-}} \frac{1}{\epsilon} \frac{1}{B(\eta \to \gamma\gamma)}, \qquad (2)$$

where $N_{\rm obs}$ is the number of $f_1(1285)$ mesons obtained in the fit (1255 ± 70), $N_{\tau^+\tau^-}$ is the number of τ pairs obtained from the luminosity and $e^+e^- \to \tau^+\tau^-$ cross section, ϵ is the efficiency for selecting a $\tau^- \to f_1(1285)\pi^-\nu_\tau$ event $(4.08 \pm 0.07)\%$, and $B(\eta \to \gamma\gamma)$ is the $\eta \to \gamma\gamma$ branching fraction (0.3943 ± 0.0026) [15]. The $\tau^- \to f_1(1285)\pi^-\nu_\tau$ branching fraction is determined by dividing Eq. (2) by the $f_1(1285) \to \eta\pi^-\pi^+$ rate (0.35 ± 0.11) [15].

The branching fractions for the $\tau^- \to f_1(1285)\pi^-\nu_\tau \to \eta\pi^-\pi^+\pi^-\nu_\tau$ and $\tau^- \to f_1(1285)\pi^-\nu_\tau$ modes are $(1.11 \pm 0.06 \pm 0.05) \times 10^{-4}$ and $(3.19 \pm 0.18 \pm 0.16 \pm 0.99) \times 10^{-4}$ respectively, where the first error is statistical and the second is systematic. The third error quoted on the $\tau^- \to f_1(1285)\pi^-\nu_\tau$ measurement is due to the large error on the $f_1(1285) \to \eta\pi^-\pi^+$ branching fraction. Most systematic errors for these branching fractions are common to the ones listed for the inclusive measurement. While the η fit uncertainty affects the inclusive result only, an extra systematic error of 1% comes through the $f_1(1285)$ decay

modeling due to the uncertainty of the branching fractions of the $f_1(1285) \to a_0(980)\pi$ and $f_1(1285) \to \eta\pi^-\pi^+$ decay modes [15]. This is determined by varying the relative contribution of the two modes within the quoted uncertainties.

The fraction of the $\tau^- \to f_1(1285)\pi^-\nu_\tau \to \eta\pi^-\pi^+\pi^-\nu_\tau$ mode to the inclusive $\tau^- \to \eta\pi^-\pi^+\pi^-\nu_\tau$ mode is found to be $0.69 \pm 0.01 \pm 0.05$ where the first error is statistical and the second is systematic (taking into account the correlations between the various components).

C. Limit on the $\tau^- \to \eta'(958)\pi^-\nu_\tau$ branching fraction

A limit on the $\tau^- \to \eta'(958)\pi^-\nu_\tau$ branching fraction can be set by searching for decays of the $\eta'(958)$ to the $\eta\pi^-\pi^+$ final state. This τ decay mode proceeds through a forbidden second-class current and is not expected to produce an observable signal [18].

A fit to the $\eta\pi^-\pi^+$ mass distribution is performed with a Gaussian function for the $\eta'(958)$ and a polynomial function for the background (see Fig. 4). The mean of the Gaussian is fixed to the mass of the $\eta'(958)$ meson. The width of the Gaussian distribution is fixed to the value obtained in a fit to a data sample containing a significant number of $\eta'(958)$ mesons. This data sample is created by removing all selection criteria except the loose preselection described in Sec. II.

We observe 19 ± 13 candidates which gives a $\tau^- \to \eta'(958)\pi^-\nu_\tau$ branching fraction of $(4.1 \pm 2.4) \times 10^{-6}$ where the error is statistical. To set a limit, we treat all of the events in the $\eta'(958)$ peak as signal; in particular, the branching fraction of the allowed $\tau^- \to \eta'(958)K^-\nu_\tau$ channel is assumed to be zero. We assume that the efficiency for selecting $\tau^- \to \eta'(958)\pi^-\nu_\tau$ events is the same as the $\tau^- \to f_1(1285)\pi^-\nu_\tau$ selection efficiency. The systematic uncertainty is dominated by a 7% error due to the uncertainty in the mass resolution of the $\eta'(958)$. The remaining systematic errors are the same as those described in the previous section. The results give a 90% confidence level upper limit on the $\tau^- \to \eta'(958)\pi^-\nu_\tau$ branching fraction of 7.2×10^{-6}.

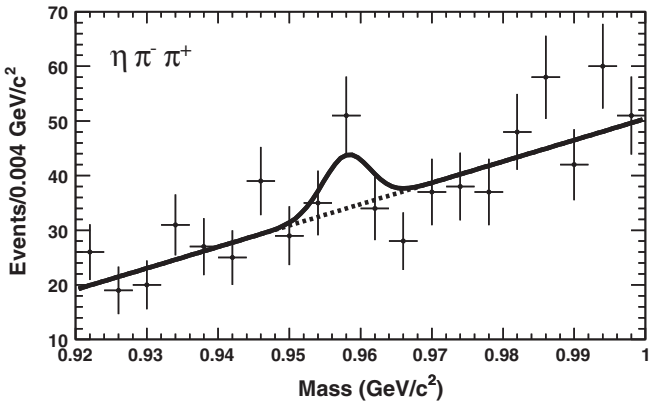

FIG. 4. Fit to the $\eta'(958)$ region of the $\eta\pi^-\pi^+$ invariant mass spectrum. The fit uses a Gaussian distribution for the peak summed with a linear function for the background. The events are tagged with muons or electrons and all selection criteria have been applied.

IV. SUMMARY

The $\tau^- \to \eta\pi^-\pi^+\pi^-\nu_\tau$ decay using the $\eta \to \gamma\gamma$ mode is studied with the *BABAR* detector. It is found that $\tau^- \to f_1(1285)\pi^-\nu_\tau$ is the dominant decay mode for the $\eta\pi^-\pi^+\pi^-$ final state.

The branching fraction of $\tau^- \to \eta\pi^-\pi^+\pi^-\nu_\tau$ is measured to be $(1.60 \pm 0.05 \pm 0.11) \times 10^{-4}$ where the first error is statistical and the second systematic. This measurement is more precise than the CLEO result $(2.3 \pm 0.5) \times 10^{-4}$ [19].

The branching fraction of the $\tau^- \to f_1(1285)\pi^-\nu_\tau \to \eta\pi^-\pi^+\pi^-\nu_\tau$ decay mode is measured to be $(1.11 \pm 0.06 \pm 0.05) \times 10^{-4}$ and is consistent with previous results [15].

The branching fraction of $\tau^- \to f_1(1285)\pi^-\nu_\tau$ is measured to be $(3.19 \pm 0.18 \pm 0.16 \pm 0.99) \times 10^{-4}$. The first error is statistical, the second is systematic, and the third error is associated with the 30% uncertainty on the $f_1 \to \eta\pi^-\pi^+$ branching fraction [15]. This measurement is in agreement with the CLEO result of $5.8^{+1.4}_{-1.3} \times 10^{-4}$ [2] and the *BABAR* result of $(3.9 \pm 0.7 \pm 0.5) \times 10^{-4}$ [3]. The branching fraction of $\tau^- \to f_1(1285)\pi^-\nu_\tau$ is predicted by effective chiral theory to be 2.9×10^{-4} [20].

A 90% confidence level upper limit on the branching fraction of the $\tau^- \to \eta'(958)\pi^-\nu_\tau$ decay is measured to be 7.2×10^{-6}. This is an order of magnitude lower than the previous 90% confidence level upper limit of 7.4×10^{-5} set by the CLEO Collaboration [2]. No significant evidence for this second-class current decay mode of the τ is observed.

ACKNOWLEDGMENTS

We are grateful for the extraordinary contributions of our PEP-II colleagues in achieving the excellent luminosity and machine conditions that have made this work possible. The success of this project also relies critically on the expertise and dedication of the computing organizations that support *BABAR*. The collaborating institutions wish to thank SLAC for its support and the kind hospitality extended to them. This work is supported by the US Department of Energy and National Science Foundation, the Natural Sciences and Engineering Research Council (Canada), the Commissariat à l'Energie Atomique and Institut National de Physique Nucléaire et de Physique des Particules (France), the Bundesministerium für Bildung und Forschung and Deutsche Forschungsgemeinschaft (Germany), the Istituto Nazionale di Fisica Nucleare (Italy), the Foundation for Fundamental Research on Matter (The Netherlands), the Research Council of Nor-

way, the Ministry of Science and Technology of the Russian Federation, Ministerio de Educación y Ciencia (Spain), and the Science and Technology Facilities Council (United Kingdom). Individuals have received support from the Marie-Curie IEF program (European Union) and the A. P. Sloan Foundation.

[1] Charge conjugation is assumed throughout this paper.
[2] T. Bergfeld *et al.* (CLEO Collaboration), Phys. Rev. Lett. **79**, 2406 (1997).
[3] B. Aubert *et al.* (*BABAR* Collaboration), Phys. Rev. D **72**, 072001 (2005).
[4] S. Banerjee, B. Pietrzyk, J. M. Roney, and Z. Was, Phys. Rev. D **77**, 054012 (2008).
[5] B. Aubert *et al.* (*BABAR* Collaboration), Nucl. Instrum. Methods Phys. Res., Sect. A **479**, 1 (2002).
[6] B. F. Ward, S. Jadach, and Z. Was, Nucl. Phys. B, Proc. Suppl. **116**, 73 (2003).
[7] S. Jadach, Z. Was, R. Decker, and J. H. Kühn, Comput. Phys. Commun. **76**, 361 (1993).
[8] T. Sjostrand, Comput. Phys. Commun. **82**, 74 (1994).
[9] E. Barberio and Z. Was, Comput. Phys. Commun. **79**, 291 (1994).
[10] D. J. Lange, Nucl. Instrum. Methods Phys. Res., Sect. A **462**, 152 (2001).
[11] S. Agostinelli *et al.* (GEANT4 Collaboration), Nucl. Instrum. Methods Phys. Res., Sect. A **506**, 250 (2003).
[12] S. Brandt *et al.*, Phys. Lett. **12**, 57 (1964); E. Farhi, Phys. Rev. Lett. **39**, 1587 (1977).
[13] R. Sobie, Nucl. Phys. B, Proc. Suppl. **144**, 15 (2005).
[14] The Novosibirsk function is defined as $f(m) = A\exp(-0.5\{\ln^2[1 + \Lambda\tau\cdot(m - m_0)]/\tau^2 + \tau^2\})$, where $\Lambda = \sinh(\tau\sqrt{\ln 4})/(\sigma\tau\sqrt{\ln 4})$, the peak position is m_0, the width is σ, and τ is the tail parameter.
[15] Y.-M. Yao *et al.* (Particle Data Group), J. Phys. G **33**, 1 (2006).
[16] M. Bishai *et al.* (CLEO Collaboration), Phys. Rev. Lett. **82**, 281 (1999).
[17] The functional form of the P-wave Breit-Wigner function is identical to the nominal Breit-Wigner function except that the width Γ_{f_1} is modified by a $(p(x)/p(0))^3$ factor. The momentum terms $p(x)$ and $p(0)$ are the momenta of the outgoing particles in a two-body decay $[f_1 \to \pi^- a_0^+(980)]$ evaluated at the current (x) and peak (m_{f_1}) mass values.
[18] H. Neufeld and H. Rupertsberger, Z. Phys. C **68**, 91 (1995).
[19] A. Anastassov *et al.* (CLEO Collaboration), Phys. Rev. Lett. **86**, 4467 (2001).
[20] B. A. Li, Phys. Rev. D **55**, 1436 (1997).